Physics Letters B 731 (2014) 342–349

Contents lists available at ScienceDirect

Physics Letters B

www.elsevier.com/locate/physletb

The general property of dynamical quintessence field

Yungui Gong [a,b,*]

[a] MOE Key Laboratory of Fundamental Quantities Measurement, School of Physics, Huazhong University of Science and Technology, Wuhan 430074, China
[b] Institute of Theoretical Physics, Chinese Academy of Sciences, Beijing 100190, China

ARTICLE INFO

Article history:
Received 21 February 2014
Received in revised form 6 March 2014
Accepted 7 March 2014
Available online 13 March 2014
Editor: J. Hisano

ABSTRACT

We discuss the general dynamical behaviors of quintessence field, in particular, the general conditions for tracking and thawing solutions are discussed. We explain what the tracking solutions mean and in what sense the results depend on the initial conditions. Based on the definition of tracking solution, we give a simple explanation on the existence of a general relation between w_ϕ and Ω_ϕ which is independent of the initial conditions for the tracking solution. A more general tracker theorem which requires large initial values of the roll parameter is then proposed. To get thawing solutions, the initial value of the roll parameter needs to be small. The power-law and pseudo-Nambu Goldstone boson potentials are used to discuss the tracking and thawing solutions. A more general w_ϕ–Ω_ϕ relation is derived for the thawing solutions. Based on the asymptotical behavior of the w_ϕ–Ω_ϕ relation, the flow parameter is used to give an upper limit on w'_ϕ for the thawing solutions. If we use the observational constraint $w_{\phi 0} < -0.8$ and $0.2 < \Omega_{m0} < 0.4$, then we require $n \lesssim 1$ for the inverse power-law potential $V(\phi) = V_0(\phi/m_{pl})^{-n}$ with tracking solutions and the initial value of the roll parameter $|\lambda_i| < 1.3$ for the potentials with the thawing solutions.

1. Introduction

The recent cosmic acceleration observed by type Ia supernova data [1] was usually explained by introducing a dynamical scalar field called quintessence [2–4]. More general dynamical scalar field models such as phantom [5], quintom [6], tachyon [7] and k-essence [8] were also proposed. For a recent review of dark energy, please see Ref. [9].

For a dynamical scalar field ϕ with the potential $V(\phi)$ in the flat Friedmann–Lemaître–Robertson–Walker universe with the metric $ds^2 = -dt^2 + a^2(t)(dr^2 + r^2\,d\theta^2 + r^2\sin^2\theta\,d\phi^2)$, its energy density and pressure are $\rho_\phi = \dot\phi^2/2 + V(\phi)$ and $p_\phi = \dot\phi^2/2 - V(\phi)$, where $\dot\phi = d\phi/dt$. The scalar field rolls down a very shallow potential while its equation of state $w_\phi = p_\phi/\rho_\phi$ approaches -1 and it starts to dominate the Universe recently. Because the scalar field catches up the background only recently and the current value of its equation of state parameter is around -1, w_ϕ does not change too much in the redshift range $0 \leqslant z < 1$ for most scalar fields, so the time variation of w_ϕ is bounded for the thawing and freezing models [10–18]. In general, the evolution of scalar field depends on the initial conditions. However, the attractor solutions and the tracking solutions are independent of the initial conditions [19–36]. In particular, the tracker field ϕ tracks below the background density for most of the history of the Universe until it starts to dominate recently for a wide range of initial conditions, and there exists a relation between w_ϕ and the fractional energy density $\Omega_\phi = 8\pi G\rho_\phi/(3H^2)$ today, where the Hubble parameter $H(t) = \dot a/a$. There also exists a general w_ϕ–Ω_ϕ relation for the thawing solutions which is well approximated by some analytical expressions [37–47]. In this Letter, we will discuss the general dynamics such as the w_ϕ–Ω_ϕ relation and the bound on $w'_\phi = dw_\phi/d\ln a$ of the tracking and thawing fields. We use the power-law potential and the pseudo-Nambu Goldstone boson (PNGB) potential [48–52] as examples to illustrate the general dynamical behaviors of tracking and thawing fields.

If the Universe is filled with the quintessence field and the background matter with the equation of state $w_b = [(1/3)a_{eq}/a]/[1 + a_{eq}/a]$, where $a_{eq} = 1/3403$ [53] is the scale factor $a(t)$ at the matter-radiation equality, then in terms of the dimensionless variables,

$$x = \frac{\phi'}{\sqrt{6}} = \frac{1}{\sqrt{6}}\frac{d\phi}{d\ln a}, \qquad y = \sqrt{\frac{V}{3H^2}},$$
$$\lambda = -\frac{V_{,\phi}}{V} = -\frac{1}{V}\frac{dV}{d\phi}, \qquad \Gamma = \frac{VV_{,\phi\phi}}{V_{,\phi}^2}, \tag{1}$$

* Correspondence to: MOE Key Laboratory of Fundamental Quantities Measurement, School of Physics, Huazhong University of Science and Technology, Wuhan 430074, China.
E-mail address: yggong@mail.hust.edu.cn.

http://dx.doi.org/10.1016/j.physletb.2014.03.013

the cosmological equations are

$$x' = \sqrt{\frac{3}{2}}\lambda y^2 + \frac{3}{2}x\left(x^2 - y^2 - 1\right) + \frac{3}{2}w_b x\left(1 - x^2 - y^2\right), \tag{2}$$

$$y' = -\sqrt{\frac{3}{2}}\lambda xy + \frac{3}{2}y\left(1 + x^2 - y^2\right) + \frac{3}{2}w_b y\left(1 - x^2 - y^2\right), \tag{3}$$

$$\lambda' = -\sqrt{6}\lambda^2(\Gamma - 1)x. \tag{4}$$

The fractional energy density and the equation of state of the scalar field are

$$\Omega_\phi = x^2 + y^2, \qquad w_\phi = \frac{x^2 - y^2}{x^2 + y^2}. \tag{5}$$

Using the fractional energy density Ω_ϕ and the parameter $\gamma = 1 + w$, Eqs. (2)–(4) become

$$\Omega_\phi' = 3(\gamma_b - \gamma_\phi)\Omega_\phi(1 - \Omega_\phi), \tag{6}$$

$$\gamma_\phi' = (2 - \gamma_\phi)\left(-3\gamma_\phi + |\lambda|\sqrt{3\gamma_\phi\Omega_\phi}\right), \tag{7}$$

$$\lambda' = -\sqrt{3\gamma_\phi\Omega_\phi}\lambda|\lambda|(\Gamma - 1). \tag{8}$$

From Eq. (7), we get a lower limit $w_\phi' \geqslant -3(1 + w_\phi)(1 - w_\phi)$. If the tracker parameter Γ can be expressed as a function of the roll parameter λ, then the above system (6)–(8) becomes an autonomous system. In this case, we have additional critical point $\Omega_{\phi c} = 1$ and $\gamma_c = 0$ which is absent in the system (2)–(4), where the subscript c means the critical point. At the point $x = 0$ and $y = 1$, the transformation from (x, y) to (Ω_ϕ, γ) is singular, so we get different critical points. Only when $\lambda_c = 0$, the point $x = 0$ and $y = 1$ is the critical point of the system (2)–(4). For the exponential potential, the point $x = 0$ and $y = 1$ is not a critical point for the system (2)–(4) and the critical point $\Omega_{\phi c} = 1$ and $\gamma_c = 0$ for the system (6)–(8) is not a stable point.

If we use the flow parameter $F = \gamma_\phi/(\Omega_\phi\lambda^2)$ [16], then Eq. (7) can be written as

$$\gamma_\phi' = 3\gamma_\phi(2 - \gamma_\phi)(-1 + 1/\sqrt{3F}). \tag{9}$$

To understand the general dynamics of the quintessence, it is useful to use the function $\beta = \ddot{\phi}/(3H\dot{\phi})$ [16,44],

$$\beta = -1 + \frac{1 - w_\phi}{\sqrt{12F}} = \frac{1}{2}\left[\Omega_\phi\gamma_\phi + (1 - \Omega_\phi)\gamma_b\right] - \frac{\beta'}{3(1 + \beta)} - \frac{V_{,\phi\phi}}{9(1 + \beta)H^2}. \tag{10}$$

For the thawing solution, the quintessence field rolls down the potential very slowly, $V_{,\phi\phi} \approx 0$ and β is almost a constant, so $\beta \approx \gamma_b/2$ at early time when $\Omega_\phi \approx 0$ and $w_\phi \approx -1$ [44].

2. Tracker solution

The energy density of the tracker field ϕ tracks below the background density for most of the history of the Universe, it starts to dominate the energy density only recently and then drives the cosmic acceleration. The tracker fields have attractor-like solutions in the sense that they rapidly converge to a common cosmic evolutionary track of $\rho_\phi(t)$ and $w_\phi(t)$ for a very wide range of initial conditions, so the tracking solutions are extremely insensitive to the initial conditions [4,22]. Furthermore, an important relation between w_ϕ and Ω_ϕ today was found for the tracker field. When the tracker field enters the tracking solution, it satisfies the tracker condition [22]

$$\gamma_\phi = 1 + w_\phi = \frac{1}{3}\lambda^2\Omega_\phi, \tag{11}$$

thus this condition is the initial condition of tracking solution. In other words, the initial condition for the tracking solution reads $F = 1/3$. From Eq. (7), we see that $\gamma_\phi' = 0$ when the tracker condition is satisfied, so it is possible that w_ϕ stops varying. On the other hand, the quintessence field satisfies the tracker equation [22,28]

$$\Gamma - 1 = \frac{3(w_b - w_\phi)(1 - \Omega_\phi)}{(1 + w_\phi)(6 + \tilde{x}')} - \frac{(1 - w_\phi)\tilde{x}'}{2(1 + w_\phi)(6 + \tilde{x}')} - \frac{2\tilde{x}''}{(1 + w_\phi)(6 + \tilde{x}')^2}, \tag{12}$$

where $\tilde{x} = \ln[(1 + w_\phi)/(1 - w_\phi)]$ and $\tilde{x}' = d\ln\tilde{x}/d\ln a$. For the tracking solution, w_ϕ is nearly constant, so $\tilde{x}' \approx \tilde{x}'' \approx 0$, and we get

$$w_\phi \approx \frac{w_b(1 - \Omega_\phi) - 2(\Gamma - 1)}{2\Gamma - 1 - \Omega_\phi} < w_b \quad (\Gamma > 1). \tag{13}$$

If $\Omega_\phi \approx 0$ when the tracker condition (11) is satisfied, then

$$w_\phi = w_\phi^{trk} = \frac{w_b - 2(\Gamma - 1)}{2\Gamma - 1}, \tag{14}$$

and $\beta = -\gamma_b/2(2\Gamma - 1)$ are approximately constants if the tracker parameter Γ is nearly constant, $\Omega_\phi \propto a^{6\gamma_b(\Gamma-1)/(2\Gamma-1)}$ increases with time and $\lambda^2 \approx 3(1 + w_\phi^{trk})/\Omega_\phi$ decreases with time. For the tracker field, $V_{,\phi\phi}/H^2$ is not negligible, so $\beta \neq \gamma_b/2$. In fact, $V_{,\phi\phi}/H^2$ is a constant for the exponential potential when the attractor is reached.

If Ω_ϕ is not small or the tracker parameter changes rapidly when the tracker condition (11) is satisfied, then w_ϕ won't keep to be a time independent constant and it decreases with time while Ω_ϕ increases to 1, so the scalar field does not track the background and Eq. (14) does not hold when the tracker condition (11) is satisfied, but the scalar field has the freezing behavior with $w_\phi \to -1$ asymptotically. Therefore, both the tracker condition (11) and Eq. (14) will be violated when Ω_ϕ is not negligible or Γ changes rapidly, and w_ϕ keeps decreasing.

For the tracker field, the tracking solution at late times has the property that $\gamma_\phi \to 0$ and $\Omega_\phi \to 1$, so γ_ϕ should decrease with time while Ω_ϕ increases with time. When γ_ϕ reaches the background value γ_b, and λ^2 decreases to the value $\lambda^2 = 3\gamma_\phi/\Omega_\phi$, then we reach the tracker condition. After that, γ_ϕ decreases toward to zero and Ω_ϕ increases toward 1. From Eq. (7), we know that we should keep $|\lambda| < \sqrt{3\gamma_\phi/\Omega_\phi}$ in order that $\gamma_\phi' < 0$, therefore $|\lambda|$ should decrease with time and $\lambda \to 0$ when $\gamma_\phi \to 0$. For any quintessence field rolling down its potential, $|\lambda|$ does not increase with time is equivalent to $\Gamma \geqslant 1$ as easily seen from Eq. (8).

For the exponential potential, λ is a constant and $\Gamma = 1$. If λ is small, then eventually γ_ϕ will decrease to be less than γ_b, and Ω_ϕ will quickly increase to be 1. In particular, if $\lambda^2 < 3\gamma_b$, then the system will reach the attractor solution with $\Omega_\phi = 1$ and $\gamma_\phi = \lambda^2/3$. If λ is big, i.e., $\lambda^2 \geqslant 3\gamma_b$, then the attractor solution is $\gamma_\phi = \gamma_b = \lambda^2\Omega_\phi/3$. Since the above attractors satisfy the tracker condition (11), so both of them are also tracking solutions. In Fig. 1, we show the phase diagram for the exponential potential with $\lambda = 2.1$. The original tracking solution found in [22] is independent of the value of λ which is in contradiction with the results for the exponential potential. The contradiction was then resolved in [28] by deriving the correct tracker equation (12).

With the dynamical Eqs. (6)–(8), we can understand the general dynamical evolution of the tracker field as follows: (a) Initially if $\Omega_{\phi i}$ is not too small or λ_i is large enough so that $\lambda_i^2 > 3\gamma_{\phi i}/\Omega_{\phi i}$, where the subscript i means the initial value, then γ_ϕ will increase toward 2 independent of the initial value of w_ϕ. Once $\gamma_\phi > \gamma_b$,

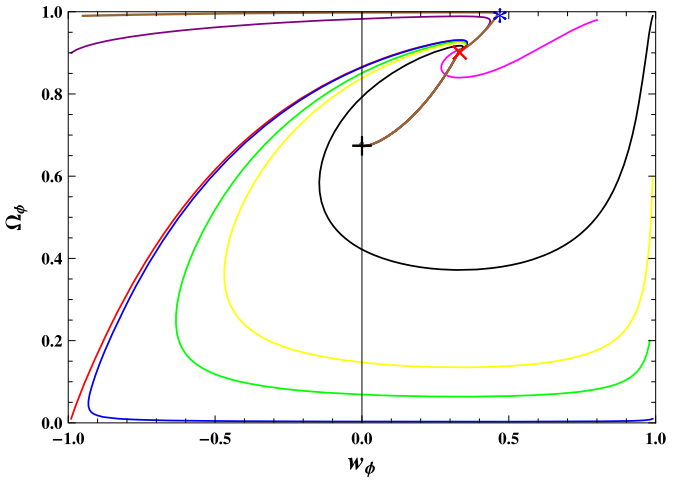

Fig. 1. The phase diagram of w_ϕ and Ω_ϕ for the exponential potential with $\lambda = 2.1$. "$*$" corresponds to the saddle node $\Omega_\phi = 1$ and $\gamma_\phi = \lambda^2/3$, "$\times$" and "$+$" correspond to the stable points $\gamma_\phi = \gamma_b$ and $\Omega_\phi = 3\gamma_\phi/\lambda^2$ with $\gamma_b = 4/3$ and $\gamma_b = 1$ respectively.

Ω_ϕ will decrease. When Ω_ϕ decreases to be small enough so that $\lambda^2 < 3\gamma_\phi/\Omega_\phi$, γ_ϕ decreases toward -1 and Ω_ϕ starts to increase once $\gamma_\phi < \gamma_b$. Even if λ decreases, it will overtake $3\gamma_\phi/\Omega_\phi$ when $\gamma_\phi \to 0$, then γ_ϕ increases again. Once γ_ϕ increases away from zero, we will have $\lambda^2 < 3\gamma_\phi/\Omega_\phi$ and the tracker behavior of w_ϕ will be reached, maybe after several oscillations. If λ_i is small, then to satisfy the tracker condition, $\Omega_{\phi i}$ cannot be too small and Ω_ϕ may reach 1 very quickly and the tracker solution with nearly constant w_ϕ will not appear. (b) Initially if $\Omega_{\phi i}$ or λ_i is small so that $\lambda_i^2 < 3\gamma_{\phi i}/\Omega_{\phi i}$, then γ_ϕ decreases toward 0 and Ω_ϕ starts to increase once $\gamma_\phi < \gamma_b$ independent of the initial value $\gamma_{\phi i}$. After that, the dynamics is similar to that in case (a). In this case, even though $\Omega_{\phi i}$ is small, but it always increases if λ_i is small, Ω_ϕ will reach 1 soon and the tracker solution with nearly constant w_ϕ does not appear. Of course, the current values of Ω_ϕ, λ and w_ϕ depend on their initial values. From these analyses, we conclude that if the initial value of λ is small, then no tracker solution with nearly constant w_ϕ appears because Ω_ϕ reaches 1 too soon. For small λ_i, once Ω_ϕ reaches 1, the equation for Ω_ϕ decouples from the dynamical system (6)–(8). Therefore, the solution to Eqs. (7) and (8) gives a relation between w_ϕ and λ. Since w_ϕ approaches -1 asymptotically, the relation is universal if Γ is a function of λ in the sense that it does not depend on the initial conditions, therefore the w_ϕ–w'_ϕ relation is also universal when $w_\phi \to -1$.

For the tracking solution, the conditions (11) and (14) are the initial conditions, so for the same initial value of Ω_ϕ at the start of the tracking solution, the trajectories of w_ϕ, Ω_ϕ an λ will be the same, that is why we have the same w_ϕ–Ω_ϕ trajectory for the tracking solution independent of the initial conditions. However, the exact values of w_ϕ and Ω_ϕ at a moment (for instance, at the present) still depend on the initial conditions. *We refer the tracking solutions as those solutions which have a common w_ϕ–Ω_ϕ trajectory for a wide range of initial conditions, technically, the tracking solutions satisfy the two conditions (11) and (14) initially.*

In [17], the author rephrased the tracker theorem as: the tracker property appears for any scalar field model in which the roll parameter λ is capable of taking on large initial values in the early Universe. If λ decreases with time, then λ is capable of taking on large initial values in the early Universe. However, for the power-law potential ϕ^α with $\alpha > 0$, the roll parameter λ can be large if we start from small ϕ, and there is no tracking solution. Furthermore, it is not clear how large the initial value should be. Therefore, we propose the tracker theorem as: *the tracker behavior appears for any quintessence field in which the roll parameter $|\lambda|$ does not increase with time and the initial value of λ should be big enough so that Ω_ϕ is still negligible when the tracker condition (11) is satisfied.* The new definition of the tracking solution and the tracker theorem proposed here are parts of the main results of this Letter.

3. Power-law potential

In this section, we use the power-law potential as an example to explicitly show the analyses presented in the previous section. Here we focus on the tracking and thawing behaviors and the bound on w'_ϕ. For the power-law potential $V(\phi) = V_0(\phi/m_{pl})^\alpha$ with the energy scale $V_0 \sim (10^{-3}\ \text{eV})^4$ and the Planck mass $m_{pl} = 1/(8\pi G)^{1/2}$, the tracker parameter $\Gamma = 1 - \alpha^{-1}$, so the dynamical system becomes an autonomous system. The dynamical analysis of the system (2)–(4) with $f(\lambda) = -1/\alpha$ was carried out in [33]. The dynamical system (2)–(4) has the following critical points: $(x_c, y_c, \lambda_c) = (\pm 1, 0, 0)$, $(x_c, y_c) = (0, 0)$ with λ arbitrary, and $(x_c, y_c, \lambda_c) = (0, 1, 0)$. Only the critical point $(x_c, y_c, \lambda_c) = (0, 1, 0)$ can be stable if $f(\lambda = 0) > 0$. For the inverse power-law potential, $f(0) = -1/\alpha > 0$, so the critical point $(x_c, y_c, \lambda_c) = (0, 1, 0)$ which corresponds to the solution $\Omega_{\phi c} = 1$ and $\gamma_{\phi c} = 0$ is a stable point. From this analysis, we know that λ will decrease to zero for the tracking solution.

3.1. Tracking solution

If we use the dynamical system (6)–(8), the critical points are: $\Omega_{\phi c} = 0$, $\gamma_{\phi c} = 0$ or $\gamma_{\phi c} = 2$ with arbitrary λ; $\Omega_{\phi c} = 1$ and $\gamma_{\phi c} = 0$ with arbitrary λ; and $(\Omega_{\phi c}, \gamma_{\phi c}, \lambda_c) = (1, 2, 0)$. The critical point $(\Omega_{\phi c}, \gamma_{\phi c}, \lambda_c) = (1, 0, 0)$ is a stable point. For the critical point $(\Omega_{\phi c}, \gamma_{\phi c}, \lambda_c) = (1, 0, 0)$, the linear approximation of the system (6)–(8) is

$$\delta\Omega'_\phi = -3\gamma_b \delta\Omega_\phi, \tag{15}$$

$$\delta\gamma'_\phi = -6\delta\gamma_\phi, \tag{16}$$

$$\delta\lambda' = 0. \tag{17}$$

One of the eigenvalues is 0. To analyze the stability of the system, we need to understand the stability of Eq. (8) for the critical point $(\Omega_{\phi c}, \gamma_{\phi c}, \lambda_c) = (1, 0, 0)$ by using the center manifold theorem [54]. So we need to solve the following equation [54]

$$\frac{d\gamma_\phi}{d\lambda}\sqrt{3\gamma_\phi\Omega_\phi}\lambda^2/\alpha = (2 - \gamma_\phi)(-3\gamma_\phi + \lambda\sqrt{3\Omega_\phi\gamma_\phi}). \tag{18}$$

Let $\gamma_\phi(\lambda) = \gamma_2\lambda^2$, up to the order of λ^2, we get $\gamma_2 = 1/3$. Substituting $\Omega_\phi = 1$ and $\gamma_\phi = \lambda^2/3$ into Eq. (8), we get

$$\lambda' = \lambda^3/\alpha. \tag{19}$$

The system is stable if $\alpha < 0$, so the critical point $(\Omega_{\phi c}, \gamma_c, \lambda_c) = (1, 0, 0)$ of the dynamical system (6)–(8) is a stable point for the inverse power-law potential. From the above analysis, we see that asymptotically $\gamma_\phi = \lambda^2\Omega_\phi/3$ to the leading order, so this stable critical point corresponds to the late time tracking solution. In other words, the flow parameter starts with the value $F = 1/3$ and approaches the value $F = 1/3$ asymptotically for the tracking solution. The function β starts with $\beta = \alpha\gamma_b/2(2-\alpha)$ and increases to $\beta = 0$ asymptotically.

Because the dynamical system (6)–(8) is hard to solve numerically if λ_i is too large, we choose to solve the dynamical system (2)–(4) numerically for the inverse power-law potential $V(\phi) = V_0(\phi/m_{pl})^{-6}$ to illustrate the tracking behavior and the results are shown in Fig. 2. As seen from Fig. 2, the general dynamics of the tracker field follows our discussion in the previous section, and

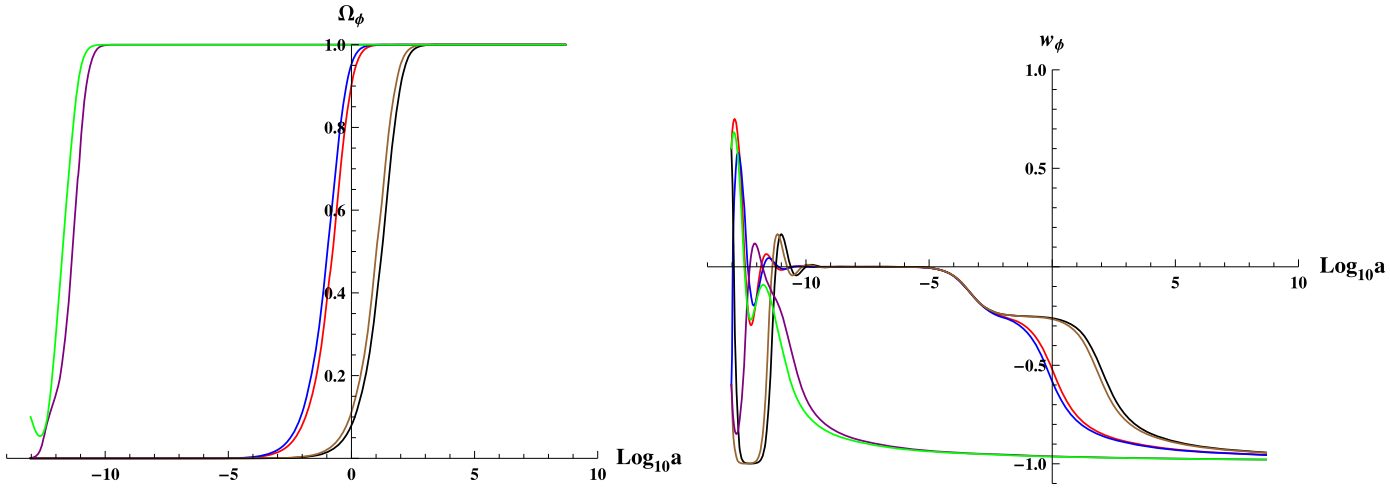

Fig. 2. The time evolutions of Ω_ϕ and w_ϕ for the inverse power-law potential $V(\phi)\sim 1/\phi^6$. The arbitrary initial time $\ln a_i=-30$ was chosen for computational convenience. The initial condition for the red line is $\Omega_{\phi i}=10^{-11}$, $w_{\phi i}=0.6$ and $\lambda_i=1.2\times 10^6$. The initial condition for the blue line is $\Omega_{\phi i}=10^{-11}$, $w_{\phi i}=-0.6$ and $\lambda_i=1.2\times 10^6$. The initial condition for the black line is $\Omega_{\phi i}=10^{-17}$, $w_{\phi i}=0.6$ and $\lambda_i=1.2\times 10^6$. The initial condition for the brown line is $\Omega_{\phi i}=10^{-17}$, $w_{\phi i}=-0.6$ and $\lambda_i=1.2\times 10^6$. The initial condition for the purple line is $\Omega_{\phi i}=10^{-3}$, $w_{\phi i}=-0.6$ and $\lambda_i=10$. The initial condition for the green line is $\Omega_{\phi i}=0.1$, $w_{\phi i}=0.6$ and $\lambda_i=10$. (For interpretation of the references to color in this figure legend, the reader is referred to the web version of this Letter.)

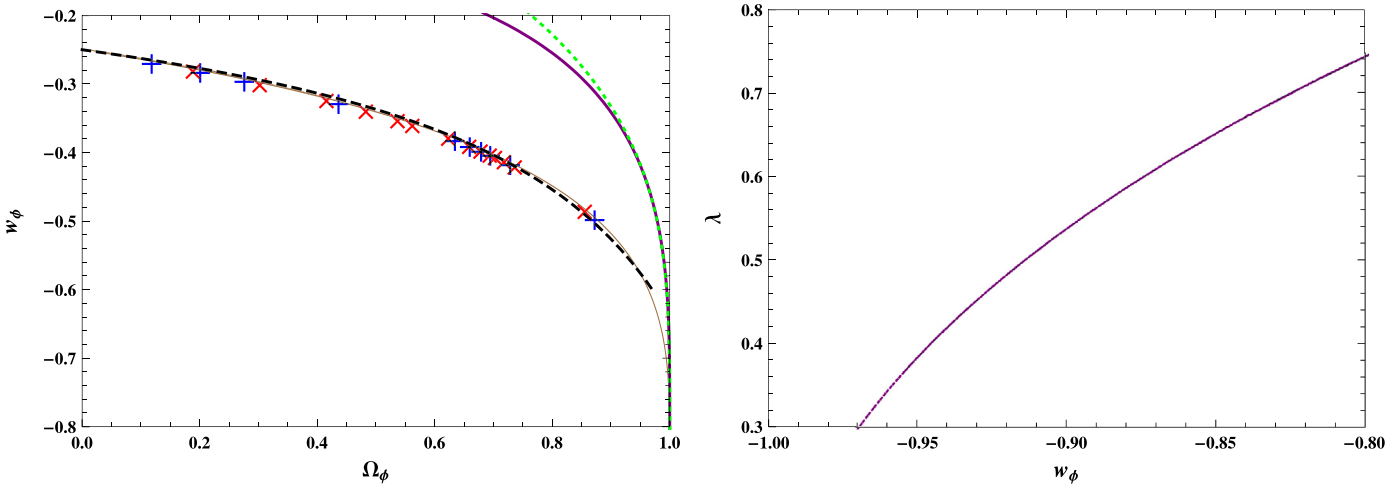

Fig. 3. The left panel shows the w_ϕ–Ω_ϕ trajectories of the evolutions of w_ϕ and Ω_ϕ shown in Fig. 2, and the right panel shows λ versus w_ϕ for the inverse power-law potential $V(\phi)\sim 1/\phi^6$ with the tracking behavior. For $\lambda_i=1.2\times 10^7$, we choose $\Omega_{\phi i}=10^{-10}$–10^{-6} and different $w_{\phi i}$. For $\lambda_i=5.2\times 10^7$, we choose $\Omega_{\phi i}=10^{-2}$–10^{-7} and different $w_{\phi i}$. The $\times$ corresponds to the points $(w_{\phi 0},\Omega_{\phi 0})$ with $\lambda_i=1.2\times 10^7$ and different $\Omega_{\phi i}$ and $w_{\phi i}$. The $+$ corresponds to the points $(w_{\phi 0},\Omega_{\phi 0})$ with $\lambda_i=5.2\times 10^7$ and different $\Omega_{\phi i}$ and $w_{\phi i}$. The dashed line is the fitting function (21). The purple and green dotted lines are for $\lambda_i=10$ without the tracking behavior. (For interpretation of the references to color in this figure legend, the reader is referred to the web version of this Letter.)

w_ϕ exhibits oscillatory behaviors before the scalar field reaches the tracking solution. For small $\lambda_i=10$ (for this case, $\lambda_i\lesssim 100$), the tracking solution with constant w_ϕ does not appear because Ω_ϕ reaches 1 in a short time. Even though the general w_ϕ–Ω_ϕ relation was not followed as shown by the dotted lines in Fig. 3, the same w_ϕ–λ and w_ϕ–w'_ϕ relations are still followed for those solutions with small λ_i when w_ϕ approaches -1. For large λ_i, the tracking behavior is realized easily. But to get the observationally allowed $\Omega_{\phi 0}$ (the subscript 0 means the current value), we need to adjust the initial values of λ, Ω_ϕ and w_ϕ. For the example shown in Fig. 2, we choose $\lambda_i=1.2\times 10^6$ and $10^{-17}\leqslant\Omega_{\phi i}\leqslant 10^{-11}$ so that $0.05\lesssim\Omega_{\phi 0}\lesssim 0.95$. We also show the relation between $w_{\phi 0}$ and $\Omega_{\phi 0}$ for the tracking solutions with different initial conditions in Fig. 3. Not only the relation between $w_{\phi 0}$ and $\Omega_{\phi 0}$ exists, but also the same relation follows for w_ϕ and Ω_ϕ at any moment after it reaches the tracking solution. This is one of the main results obtained in this Letter.

As we discussed in the previous section, the w_ϕ–Ω_ϕ trajectory is independent of the initial conditions, so the $w_{\phi 0}$–$\Omega_{\phi 0}$ relation is the same as the general w_ϕ–Ω_ϕ relation for the tracking solution because of the tracker condition, although the values of $w_{\phi 0}$ and $\Omega_{\phi 0}$ depend on the initial conditions. Therefore, we generalize the common $w_{\phi 0}$–$\Omega_{\phi 0}$ trajectory found in [4,22] to the common w_ϕ–Ω_ϕ trajectory for the tracking solutions even though w_ϕ evolves differently when the tracker field starts to dominate the Universe. The trajectory can be obtained by solving the dynamical system (6)–(8) with the initial conditions (11) and (14). A general w_ϕ–Ω_ϕ relation was proposed in [39] for slow-roll freezing quintessence by assuming constant λ as

$$\gamma_\phi=\frac{\lambda_0^2}{3}\left[\frac{1}{\sqrt{\Omega_\phi}}-\left(\frac{1}{\Omega_\phi}-1\right)\left(\tanh^{-1}(\sqrt{\Omega_\phi})+C\right)\right]^2. \tag{20}$$

Apparently, this relation cannot be applied for the tracking behavior because $\gamma_\phi\to\lambda_0^2/3$ when $\Omega_\phi\to 1$ and $\gamma_\phi\to\infty$ when $\Omega_\phi\to 0$ if $C\neq 0$. The reason why the above relation does not work is that

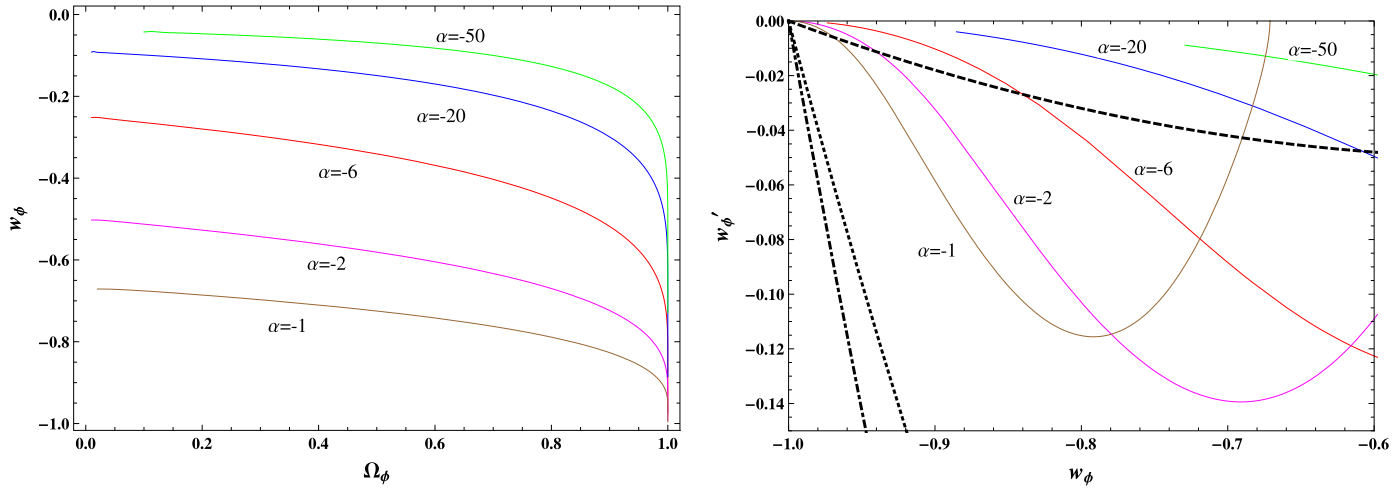

Fig. 4. The w_ϕ–Ω_ϕ and w'_ϕ–w_ϕ relations for the power-law potential $V(\phi)\sim\phi^\alpha$ with the tracking behavior. The dashed line in the right panel is for the upper limit $0.2w_\phi(1+w_\phi)$, the dotted line is for the tracking lower limit $3w_\phi(1-w_\phi^2)/(1-2w_\phi)$, and the dot-dashed line is for the freezing lower limit $3w_\phi(1+w_\phi)$.

λ is not a constant for the tracking solution as shown in Fig. 3. When Ω_ϕ is small, a linear approximation for the w_ϕ–Ω_ϕ relation was found in [29,55]. We find that the general w_ϕ–Ω_ϕ relation for $\alpha=-6$ can be fitted by the following function

$$w_\phi=\frac{w_b(1-\Omega_\phi)+0.09\Omega_\phi+0.03\Omega_\phi^2-2(\Gamma-1)}{2\Gamma-1-\Omega_\phi}. \tag{21}$$

It is obvious that w_ϕ does not differ much from the initial value (14), so w'_ϕ is small. To see how small it is, we show the w'_ϕ–w_ϕ trajectory for different α in Fig. 4. The upper limit $w'_\phi\lesssim 0.2w_\phi(1+w_\phi)$ [10] is also shown in Fig. 4. Our results show that the upper limit is violated. As we discussed above, as $w_\phi\to-1$, $F=1/3$ and $w'_\phi=0$, so we expect the violation of the upper limit $0.2w_\phi(1+w_\phi)$. The other problem is the observational constraints on the values of Ω_{m0} and $w_{\phi0}$. Since w_ϕ and Ω_ϕ follow a universal relation which is independent of the initial conditions and the energy scale V_0 of the potential, we can use the observational data to constrain the form of tracker potential. For the power-law potential $V(\phi)=V_0(\phi/m_{pl})^\alpha$, the observational constraints can be satisfied by choosing small α as shown in Fig. 4. If we choose the observational constraints $0.2\leqslant\Omega_{m0}\leqslant0.4$ and $w_0\leqslant-0.8$ [56,57], then we require $0>\alpha\gtrsim-1$.

3.2. Thawing solution

For the inverse power-law potential, if λ_i is small, then w_ϕ decreases to -1 as seen from Eq. (7). If we also fine-tune the initial value of Ω_ϕ (for $\alpha=-4$, $\Omega_{\phi i}$ is around 10^{-30} at $\ln a_i=-20$), then w_ϕ stays at the value -1 and starts to increase recently, we get the thawing behavior. From Eq. (8), it is easy to see that λ will keep to be a constant when $w_\phi=-1$. Combining Eqs. (6) and (7), we get

$$\frac{d\gamma_\phi}{d\Omega_\phi}=\frac{-3\gamma_\phi(2-\gamma_\phi)+\lambda(2-\gamma_\phi)\sqrt{3\gamma_\phi\Omega_\phi}}{3(\gamma_b-\gamma_\phi)\Omega_\phi(1-\Omega_\phi)}. \tag{22}$$

Taking the approximation $\gamma_\phi\ll1$, then Eq. (22) can be approximated as

$$\frac{d\gamma_\phi}{d\Omega_\phi}=\frac{-6\gamma_\phi+2\lambda\sqrt{3\gamma_\phi\Omega_\phi}}{3\gamma_b\Omega_\phi(1-\Omega_\phi)}. \tag{23}$$

The solution to the above Eq. (23) with constant $\lambda\approx\lambda_i$ is

$$\gamma_\phi=\frac{\lambda_i^2}{3}\left(1+\frac{1}{2}\gamma_b\right)^{-2}\Omega_\phi(1-\Omega_\phi)^{2/\gamma_b}\times{}_2F_1^2\left(\frac{1}{\gamma_b}+\frac{1}{2},\frac{1}{\gamma_b}+1,\frac{1}{\gamma_b}+\frac{3}{2};\Omega_\phi\right), \tag{24}$$

where ${}_2F_1(a,b,c,x)$ is the hypergeometric function. This approximation breaks down when $\gamma_\phi\sim1$. As $\Omega_\phi\to0$ and $w_\phi\to-1$, $\gamma_\phi\to\lambda_0^2\Omega_\phi/3(1+\gamma_b/2)^2$, so the flow parameter $F=1/3(1+\gamma_b/2)^2$ and $\beta=\gamma_b/2$ which is consistent with the result found in [44] with different argument. If w_ϕ starts to increase during the matter domination, $\gamma_b=1$ and $F=4/27$, we recover the familiar w_ϕ–Ω_ϕ relation (20) with $C=0$. We show the evolutions of Ω_ϕ, w_ϕ and λ in Fig. 5, and the w_ϕ–Ω_ϕ and w_ϕ–w'_ϕ relations are shown in Fig. 6 with dotted lines for the inverse power-law potential with $\alpha=-4$. We choose two different initial values of $\lambda_i=0.8$ and $\lambda_i=0.4$. The thawing solution was kept up to $w_\phi\sim-0.95$ for $\lambda_i=0.4$ and $w_\phi\sim-0.85$ for $\lambda_i=0.8$. When the scalar field takes the thawing solution, λ is almost a constant as shown in Fig. 5 and the analytical relation (24) approximates the w_ϕ–Ω_ϕ relation well as shown in Fig. 6. Since $\lambda'\propto\lambda^2$, the larger λ is, the faster λ changes, so the analytical relation (24) gives better approximation for smaller λ_i as shown in Fig. 6.

For the power-law potential with positive α, the roll parameter $|\lambda|$ increases with time and there is no asymptotically freezing solution. To get the thawing solution, we need to start with small $|\lambda_i|$ so that w_ϕ decreases to -1. If we also fine-tune the initial value of Ω_ϕ (for $\alpha=6$, $\Omega_{\phi i}$ is around 10^{-30} at $\ln a_i=-20$), then w_ϕ stays at the value -1 and starts to increase recently. We show the evolutions of Ω_ϕ, w_ϕ and λ in Fig. 5, the w_ϕ–Ω_ϕ and w_ϕ–w'_ϕ relations in Fig. 6 by the dashed lines for the power-law potential with $\alpha=6$. We choose two different initial values of $\lambda_i=-0.8$ and $\lambda_i=-0.4$. When the scalar field takes the thawing solution, λ is almost a constant as shown in Fig. 5 and the analytical relation (24) approximates the w_ϕ–Ω_ϕ relation well as shown in Fig. 6. Again the analytical relation (24) gives better approximation for smaller $|\lambda_i|$ as shown in Fig. 6. If we use the observational constraints $w_{\phi0}\leqslant-0.8$ and $\Omega_{\phi0}>0.6$, then the analytical relation (20) requires $|\lambda_i|<1.3$. From the analytical relation (20), we see that $\lambda\to3(1+w_\phi)/\Omega_\phi$ as $\Omega_\phi\to1$ which is not true for the positive power-law potential because $|\lambda|$ keeps increasing and it increases faster and faster once w_ϕ deviate from -1, this means

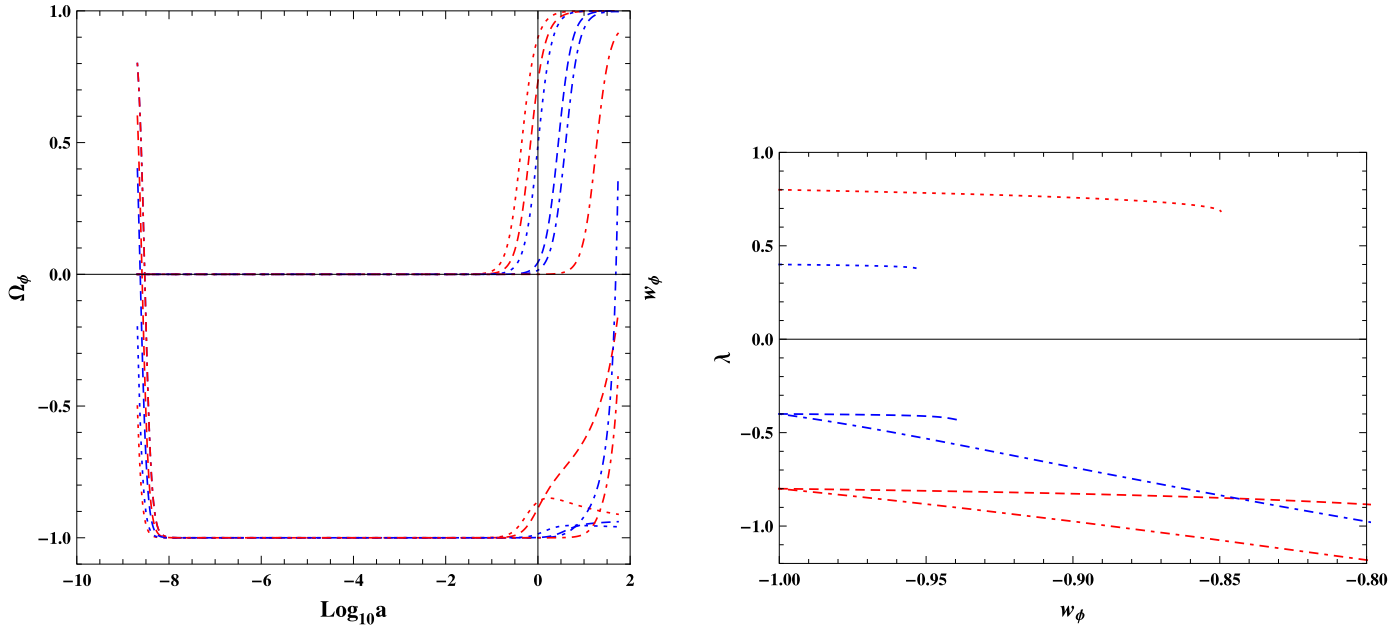

Fig. 5. The left panel shows the evolutions of Ω_ϕ and w_ϕ and the right panel shows the evolutions of λ for the thawing solutions. The arbitrary initial time $\ln a_i = -20$ was chosen for computational convenience. The red lines are for $|\lambda_i| = 0.8$ and the blue lines are for $|\lambda_i| = 0.4$. The dashed lines are for the power-law potential $V(\phi) \sim \phi^6$, the dotted lines are for the inverse power-law potential $V(\phi) \sim \phi^{-4}$, and the dot-dashed lines are for the PNGB potential. (For interpretation of the references to color in this figure legend, the reader is referred to the web version of this Letter.)

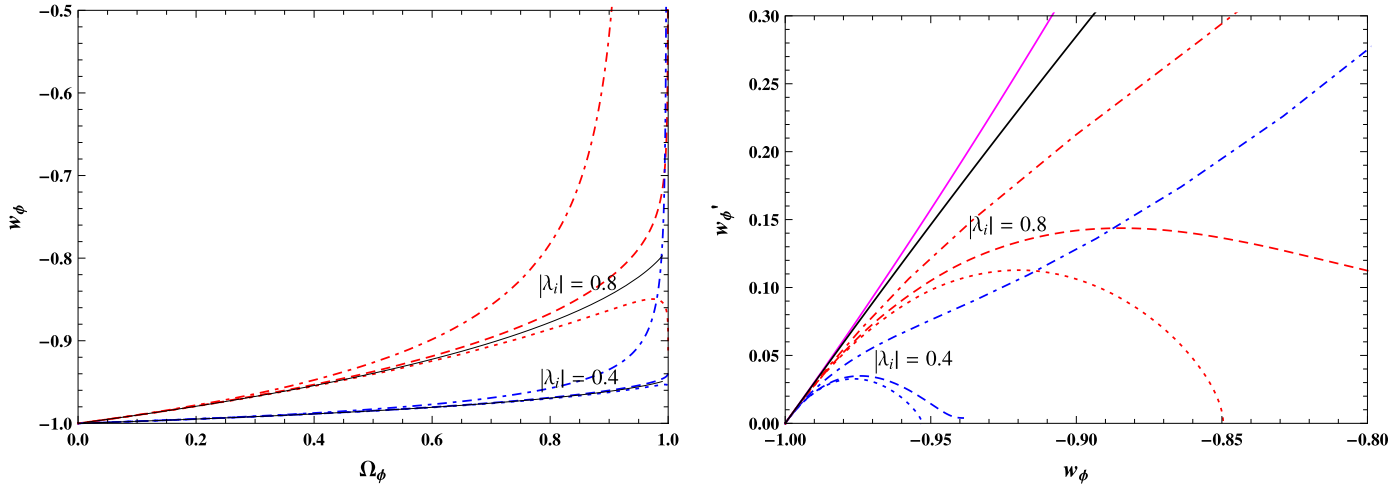

Fig. 6. The w_ϕ–Ω_ϕ and w'_ϕ–w_ϕ relations for the thawing solutions. The dashed lines are for the power-law potential $V(\phi) = \phi^6$, the dotted lines are for the inverse power-law potential $V(\phi) = \phi^{-4}$, and the dot-dashed lines are for the PNGB potential. The black lines in the left panel denote the analytical result (20) with $C = 0$. In the right panel, the magenta line denotes the upper limit $3(1 + w_\phi)(2 + w_\phi)$ for thawing models, and the black line denotes the upper limit $3(1 - w_\phi^2)/2$. (For interpretation of the references to color in this figure legend, the reader is referred to the web version of this Letter.)

that the approximation is broken as $\Omega_\phi \to 1$. On the other hand, as $\Omega_\phi \to 0$, we get $1 + w_\phi \to \lambda^2\Omega_\phi/3(1 + \gamma_b/2)^2 = 4\lambda^2\Omega_\phi/27$, so the flow parameter $F = 1/3(1 + \gamma_b/2)^2 = 4/27$ initially at the matter domination for the thawing solution and the flow parameter $F = 1/3$ when the quintessence field leaves the thawing solution. Therefore, $4/27 \leqslant F \leqslant 1/3$ for the thawing solution, we get an upper limit $w'_\phi \leqslant 3(1 - w_\phi^2)/2$ which is smaller than the upper limit $w'_\phi = 3(1 + w_\phi)(2 + w_\phi)$ [10], and there is no lower limit on w'_ϕ. As shown in Fig. 6, the lower limit $w'_\phi \geqslant 1 + w_\phi$ [10] does not hold. These two upper bounds are also shown in Fig. 6 and they are satisfied by the thawing solutions. From Eq. (10), we get $\beta = \gamma_b/2 = 1/2$ initially and $\beta = -\gamma_\phi/2$ when the thawing period ends.

4. PNGB potential

In this section, we focus on the w_ϕ–Ω_ϕ approximation (24) and the limit on w'_ϕ for the PNGB potential. The PNGB potential $V(\phi) = M^4[1 \pm \cos(N\phi/f)]$ was first proposed in the schizon model in which the small PNGB mass is protected by fermionic chiral symmetries [48,49], π meson and the axion are examples of PNGB. In cosmology, the PNGB potential was first introduced as natural inflation [50], and was later found that it also dominates the energy density of the universe at present [51]. In this Letter, we choose the PNGB potential without loss of generality, $V(\phi) = M^4[1 - \cos(\phi/m_{pl})]$ with the energy scale $M \sim 10^{-3}$ eV, the tracker parameter $\Gamma = (\lambda^2 - 1)/2\lambda^2 < 1$ and $f(\lambda) = \Gamma - 1 = -(1 + \lambda^2)/2\lambda^2$ [33], so there is no tracking solution for the PNGB potential. Since

$f(0)$ is not well defined, the dynamical analysis on the fixed points in [33] is not applicable. The critical points are: $\Omega_{\phi c}=0$, $\gamma_c=0$ or $\gamma_c=2$ with arbitrary λ; $\Omega_{\phi c}=1$ and $\gamma_c=0$ with arbitrary λ; and $(\Omega_{\phi c},\gamma_c,\lambda_c)=(1,2,0)$. In fact, all the critical points are unstable points.

In this model, $\lambda'\propto(1+\lambda)^2$, the roll parameter λ changes faster than the power-law potential, so we don't expect that the analytical expression (24) approximates the w_ϕ–Ω_ϕ as well as that for the power-law potential with the same λ_i. To get the thawing solution, we also need to start with small $|\lambda_i|$ so that w_ϕ quickly reaches the initial thawing value -1, and we also need to fine-tune the initial value of Ω_ϕ to be around 10^{-32} at $\ln a_i=-20$. The evolutions of Ω_ϕ, w_ϕ and λ are shown in Fig. 5, and the w_ϕ–Ω_ϕ and w_ϕ–w'_ϕ relations are shown in Fig. 6 with dot-dashed lines. As we expect, λ does not keep to be nearly constant, the approximation (20) is not good for large λ_i and it breaks down when Ω_ϕ approaches 1.

5. Discussion and conclusions

When the tracking solution is reached, $w'_\phi\approx w''_\phi\approx 0$, so w_ϕ is almost a constant and both the tracker condition (11) and Eq. (14) are satisfied. To keep w_ϕ to be a constant, Ω_ϕ should be small and the tracker parameter Γ should be nearly constant, so the tracker condition (11) requires the roll parameter λ to be large. Therefore, the tracker parameter $\Gamma>1$ and large initial value of the roll parameter λ are the necessary conditions for tracking solutions. Based on this analysis, we proposed the tracker theorem. Although the current value of Ω_ϕ and w_ϕ depend on the initial conditions for the tracking solutions, the w_ϕ–Ω_ϕ trajectory before Ω_ϕ reaches 1 is independent of the initial conditions and it can be used to exclude models by comparing it with the observational constraints. If we choose the observational constraints $0.2\leqslant\Omega_{m0}\leqslant 0.4$ and $w_0\leqslant -0.8$, then we require $n\lesssim 1$ for the inverse power-law potential $V(\phi)=V_0(\phi/m_{pl})^{-n}$. Since the dark energy domination ($\Omega_\phi=1, w_\phi=-1,\lambda=0$) is the attractor for the inverse power-law potential, the asymptotic behaviors of λ and w_ϕ are the same and the same asymptotic λ–w_ϕ trajectory is followed by all solutions including the tracking and non-tracking solutions. The flow parameter F starts and ends with $F=1/3$, the upper bound $0.2w_\phi(1+w_\phi)$ does not hold and we expect that no such upper bound exists for the freezing models, this will make the distinction between cosmological constant and dynamical tracker fields more difficult.

If the initial value of the roll parameter λ is small, then w_ϕ quickly decreases to -1 and stays at the value until the roll parameter λ becomes large, after that w_ϕ starts to increase. This thawing behavior can be achieved for the power-law potential with positive α and the PNGB potential. The thawing behavior can also be achieved for the inverse power-law potential for a period of time if the initial value of the roll parameter is small. In general, we need to fine-tune the initial conditions so that we get the right values of $\Omega_{\phi0}$ and $w_{\phi0}$ which are consistent with the observational constraints for the thawing solutions. Because $w_\phi\approx -1$ initially, the roll parameter changes very slowly and it can be approximated as a constant, a general w_ϕ–Ω_ϕ relation (24) is then obtained. Based on the asymptotical behavior of the w_ϕ–Ω_ϕ relation, the flow parameter $F=1/3(1+\gamma_b/2)^2=4/27$ when $\Omega_\phi\to 0$ and $w_\phi\to -1$ during the matter domination, and $F=1/3$ when the thawing behavior ends, we derive the upper bound $w'_\phi\leqslant 3(1-w_\phi^2)/2$ and we expect that no lower bound exists for the thawing models, so the distinction between cosmological constant and dynamical thawing models becomes more difficult. If we use the observational constraint $w_{\phi0}<-0.8$ and $0.2<\Omega_{m0}<0.4$, we find that the initial value of the roll parameter $|\lambda_i|<1.3$ for the potentials with the thawing solutions.

In summary, we find that the same relation not only exists between $w_{\phi0}$ and $\Omega_{\phi0}$, but also exists between w_ϕ and Ω_ϕ at any time after the tracker field takes the tracking solutions. The relation is independent of the initial conditions and the energy scale V_0 of the tracker field, so the observational data can be used to constrain the tracker model by using this relation. Based on the existence of the relation, we generalize the tracking solutions with a common track of $w_\phi(t)$ to those solutions with a common w_ϕ–Ω_ϕ trajectory and we propose the tracker theorem by using the roll parameter λ. Both the upper limit $w'_\phi<0.2w_\phi(1+w_\phi)$ for the tracking solutions and the lower limit $w'_\phi>1+w_\phi$ for the thawing solutions are found to be violated, and we propose a lower upper bound $w'_\phi\leqslant 3(1-w_\phi^2)/2$ for the thawing solutions.

Acknowledgements

This work was partially supported by the National Basic Science Program (Project 973) of China under grant No. 2010CB833004, the NNSF of China under grant Nos. 10935013 and 11175270, the Program for New Century Excellent Talents in University under grant No. NCET-12-0205 and the Fundamental Research Funds for the Central Universities under grant No. 2013YQ055.

References

[1] S. Perlmutter, et al., Nature 391 (1998) 51;
A.G. Riess, et al., Astron. J. 116 (1998) 1009;
S. Perlmutter, et al., Astrophys. J. 517 (1999) 565.
[2] B. Ratra, P. Peebles, Phys. Rev. D 37 (1988) 3406;
C. Wetterich, Nucl. Phys. B 302 (1988) 668.
[3] R. Caldwell, R. Dave, P.J. Steinhardt, Phys. Rev. Lett. 80 (1998) 1582.
[4] I. Zlatev, L.-M. Wang, P.J. Steinhardt, Phys. Rev. Lett. 82 (1999) 896.
[5] R. Caldwell, Phys. Lett. B 545 (2002) 23.
[6] B. Feng, X.-L. Wang, X.-M. Zhang, Phys. Lett. B 607 (2005) 35;
B. Feng, M. Li, Y.-S. Piao, X. Zhang, Phys. Lett. B 634 (2006) 101;
Z.-K. Guo, Y.-S. Piao, X.-M. Zhang, Y.-Z. Zhang, Phys. Lett. B 608 (2005) 177.
[7] A. Sen, J. High Energy Phys. 0207 (2002) 065;
A. Sen, J. High Energy Phys. 0204 (2002) 048;
T. Padmanabhan, Phys. Rev. D 66 (2002) 021301.
[8] C. Armendariz-Picon, V.F. Mukhanov, P.J. Steinhardt, Phys. Rev. Lett. 85 (2000) 4438.
[9] V. Sahni, A.A. Starobinsky, Int. J. Mod. Phys. D 9 (2000) 373;
E.J. Copeland, M. Sami, S. Tsujikawa, Int. J. Mod. Phys. D 15 (2006) 1753;
S. Nojiri, S.D. Odintsov, Int. J. Geom. Methods Mod. Phys. 4 (2007) 115;
T. Padmanabhan, Gen. Relativ. Gravit. 40 (2008) 529;
M. Li, X.-D. Li, S. Wang, Y. Wang, Commun. Theor. Phys. 56 (2011) 525;
S. Nojiri, S.D. Odintsov, Phys. Rep. 505 (2011) 59;
K. Bamba, S. Capozziello, S. Nojiri, S.D. Odintsov, Astrophys. Space Sci. 342 (2012) 155.
[10] R. Caldwell, E.V. Linder, Phys. Rev. Lett. 95 (2005) 141301.
[11] V. Barger, E. Guarnaccia, D. Marfatia, Phys. Lett. B 635 (2006) 61.
[12] R.J. Scherrer, Phys. Rev. D 73 (2006) 043502.
[13] E.V. Linder, Phys. Rev. D 73 (2006) 063010.
[14] T. Chiba, Phys. Rev. D 73 (2006) 063501;
T. Chiba, Phys. Rev. D 80 (2009) 129901 (Erratum).
[15] A. Ali, M. Sami, A. Sen, Phys. Rev. D 79 (2009) 123501.
[16] R.N. Cahn, R. de Putter, E.V. Linder, J. Cosmol. Astropart. Phys. 0811 (2008) 015.
[17] L.A. Urena-Lopez, J. Cosmol. Astropart. Phys. 1203 (2012) 035.
[18] X. Chen, Y. Gong, The limit on w' for tachyon dark energy, arXiv:1309.2044, 2013.
[19] P.G. Ferreira, M. Joyce, Phys. Rev. Lett. 79 (1997) 4740;
P.G. Ferreira, M. Joyce, Phys. Rev. D 58 (1998) 023503.
[20] E.J. Copeland, A.R. Liddle, D. Wands, Phys. Rev. D 57 (1998) 4686.
[21] A.R. Liddle, R.J. Scherrer, Phys. Rev. D 59 (1999) 023509.
[22] P.J. Steinhardt, L.-M. Wang, I. Zlatev, Phys. Rev. D 59 (1999) 123504.
[23] P. Brax, J. Martin, Phys. Rev. D 61 (2000) 103502.
[24] L.A. Urena-Lopez, T. Matos, Phys. Rev. D 62 (2000) 081302.
[25] S.A. Bludman, M. Roos, Phys. Rev. D 65 (2002) 043503.
[26] S. Dodelson, M. Kaplinghat, E. Stewart, Phys. Rev. Lett. 85 (2000) 5276.
[27] V.B. Johri, Phys. Rev. D 63 (2001) 103504;
V.B. Johri, Class. Quantum Gravity 19 (2002) 5959.

[28] C. Rubano, P. Scudellaro, E. Piedipalumbo, S. Capozziello, M. Capone, Phys. Rev. D 69 (2004) 103510.
[29] C.R. Watson, R.J. Scherrer, Phys. Rev. D 68 (2003) 123524.
[30] J. Aguirregabiria, R. Lazkoz, Phys. Rev. D 69 (2004) 123502.
[31] M. Sahlen, A.R. Liddle, D. Parkinson, Phys. Rev. D 75 (2007) 023502.
[32] D. Huterer, H.V. Peiris, Phys. Rev. D 75 (2007) 083503.
[33] W. Fang, Y. Li, K. Zhang, H.-Q. Lu, Class. Quantum Gravity 26 (2009) 155005.
[34] M. Szydlowski, O. Hrycyna, A. Stachowski, Int. J. Geom. Methods Mod. Phys. 11 (2014) 1460012.
[35] S. del Campo, et al., Phys. Rev. D 88 (2013) 023532.
[36] N. Roy, N. Banerjee, Gen. Relativ. Gravit. 46 (2014) 1651.
[37] R.J. Scherrer, A. Sen, Phys. Rev. D, Part. Fields 77 (2008) 083515.
[38] R.J. Scherrer, A. Sen, Phys. Rev. D, Part. Fields 78 (2008) 067303.
[39] S. Dutta, R.J. Scherrer, Phys. Lett. B 704 (2011) 265.
[40] R. Crittenden, E. Majerotto, F. Piazza, Phys. Rev. Lett. 98 (2007) 251301.
[41] S. Dutta, R.J. Scherrer, Phys. Rev. D 78 (2008) 123525.
[42] T. Chiba, S. Dutta, R.J. Scherrer, Phys. Rev. D 80 (2009) 043517.
[43] G. Gupta, E.N. Saridakis, A.A. Sen, Phys. Rev. D 79 (2009) 123013.
[44] T. Chiba, Phys. Rev. D 79 (2009) 083517.
[45] S. Sen, A. Sen, M. Sami, Phys. Lett. B 686 (2010) 1.
[46] S. del Campo, V.H. Cardenas, R. Herrera, Phys. Lett. B 694 (2011) 279.
[47] Y. Gong, Q. Gao, Eur. Phys. J. C 74 (2014) 2729.
[48] C.T. Hill, G.G. Ross, Phys. Lett. B 203 (1988) 125.
[49] C.T. Hill, G.G. Ross, Nucl. Phys. B 311 (1988) 253.
[50] K. Freese, J.A. Frieman, A.V. Olinto, Phys. Rev. Lett. 65 (1990) 3233.
[51] J.A. Frieman, C.T. Hill, A. Stebbins, I. Waga, Phys. Rev. Lett. 75 (1995) 2077.
[52] K. Coble, S. Dodelson, J.A. Frieman, Phys. Rev. D 55 (1997) 1851.
[53] P. Ade, et al., Planck 2013 results. XVI. Cosmological parameters, arXiv:1303.5076, 2013.
[54] H.K. Khalil, Nonlinear Systems, third edition, Prentice Hall, New Jersey, 2002.
[55] T. Chiba, Phys. Rev. D 81 (2010) 023515.
[56] Y. Gong, Q. Gao, Z.-H. Zhu, Mon. Not. R. Astron. Soc. 430 (2013) 3142.
[57] Q. Gao, Y. Gong, The tension on the cosmological parameters from different observational data, arXiv:1308.5627, 2013.